Journal of Visualization, Vol. 3, No. 1 (2000) 27-35

Qualitative and Quantitative Flow Visualization of Bubble Motions in a Plane Bubble Plume

Murai, Y.*[1], Matsumoto, Y.*[2] and Yamamoto, F.*[1]

*1 Department of Mechanical Engineering, Fukui University, Bunkyo, 3-9-1, Fukui 910-8507, Japan.
*2 Department of Mechanical Engineering, The University of Tokyo, Hongo 7-3-1, Tokyo 113-8656, Japan.

Received 16 November 1998.
Revised 10 September 1999.

***Abstract*:** Overall, as well as individual, bubble behavior of a plane bubble plume which is confined by two parallel plates is investigated by means of several qualitative and quantitative flow visualization methods. These include observation, measurement of time-averaged void distribution, surface tufts and particle imaging velocimetry. Several kinds of unstable motion of the bubble convection, which depend on the free surface initial height and on the gas flow rate, are observed. The bubble motion along the bubble plume is precisely measured by an image-processing method which also delivers velocity vectors, number density and size of the bubbles.

***Keywords*:** multiphase flow, bubble plume, particle imaging velocimetry (PIV).

1. Introduction

Bubble-driven convection is utilized in many industrial processes, such as chemical plants, bio-reactors and nuclear power plants. The main features of this kind of flow are the following ones; 1) large scale circulation of liquid phase can be generated in natural circulation systems like lakes, agitation tanks, and so on, 2) strong rising flows can be induced by the pumping effect as in air-lifting pumps, 3) high surface flows may develop at the free surface, by which density and transportation of surface floating substances can be controlled, 4) high turbulence energy can be produced in the two-phase region due to the strong local interaction between individual bubbles and surrounding liquid flow.

Experimental observation of this kind of flow was performed by Hussain and Siegel (1976) who reported on the relation between the gas flow rate and the liquid flux induced by large gas bubbles for the basic issue of the pumping effect. Leitch and Baines (1989) measured the liquid volume flux which was induced in a tank by a weak bubble plume. Alam and Arakeri (1993) investigated the microscopic flow structure of a plane bubble plume and observed sinuous instability due to small bubble concentration. These experimental researches, however, little described the relation between the multi-dimensionality of liquid convection and the local bubble motion.

On the other hand, during the past several years, numerical predictions for such a flow advanced very rapidly, but detailed experimental information is still required in order to evaluate the validity of their models and/or of computational methods. This is because there are still many unsettled problems regarding in particular the handling of the dispersed phase while performing numerical calculations. Therefore, local and instantaneous measurements of two-phase flow have recently become more important than in the past.

In the present investigation, at first, the transient flow pattern of a plane bubble plume in a rectangular tank is qualitatively visualized by using a bubble-illumination method and surface tufts. Then, the time averaged void distribution is calculated by image-processing the visualized image. Finally, the microscopic structure of the vertically developing bubbly flow along the bubble plume is measured by using particle imaging velocimetry (PIV)

which allows the measurement of velocity vectors, number density and size of the bubble. Experimental results reveal that the flow pattern of the bubble-driven convection in the tank is remarkably influenced by the experimental conditions such as the initial level of free surface and the gas flow rate. For example, swaying and meandering motions, as well as a stratified structure of the bubble plume, are observed. In the case of symmetrical flow in the tank, the measurements of bubble motion make clear that the initial flow profile from the bubble injector spatially evolves to a well-developed structure in the upper region.

2. Experimental Method

2.1 Experimental Set-up

The experimental apparatus is schematically shown in Fig.1(a). It consists of a rectangular tank, 900 mm high, 300 mm wide and 20 mm deep, made of acrylic resin plates which are sustained by brass frames. The bubbly flow in the tank has a nearly two dimensional structure due to the restriction of the third velocity component in the horizontal depth direction. This kind of experimental condition for bubbly flow is referred to as "pseudo two-dimensional experiment". The bubble injector, 90 mm wide and 12 mm deep is set at the center of the bottom plane, where 24 injection needles, protruding 5 mm in the tank, are fixed at equal pitches as shown in Fig.1(b). All the injection needle exit sections are set parallel to the top free surface whose level is varied from 300 mm to 900 mm. The gas flow rate and the bubble size can be varied either by regulating the differential pressure acting on the injection needles, or by changing the latter ones. Liquid and gases used, as well as experimental conditions, are shown in Table 1. The lighting to visualize the flow can be performed in the three different ways, i.e., Experiment A: Bubble-illumination method, Experiment B: Front-lighting method, and Experiment C: Back-lighting method through a light-diffusing film.

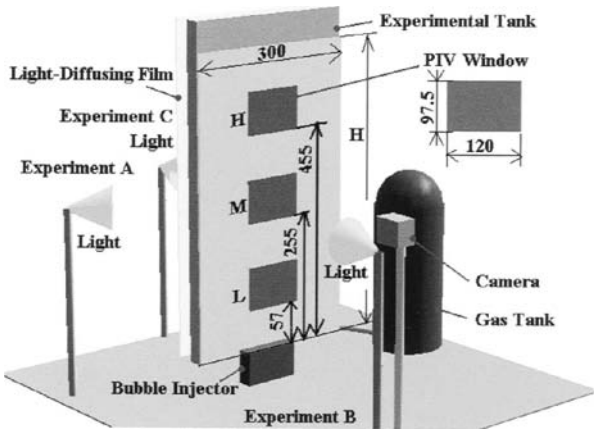

Fig. 1(a). Schematic diagram of experimental apparatus (*H*: initial height of free surface).

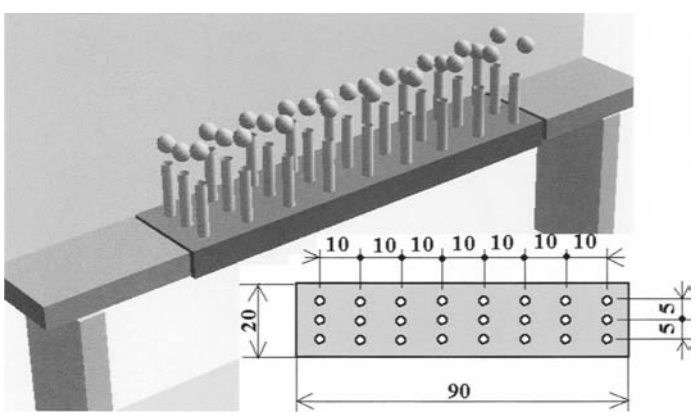

Fig. 1(b). Layout of the bubble injection needles.

Table1. Detailed conditions of the present experiments.

Experiment		Experiment A	Experiment B	Experiment C
Liquid	Density	1000 kg/m^3 (water)		960 kg/m^3 (Silicone Oil)
	Kinematic Viscosity	1.3 x 10^{-6} m^2/s		5.0 x 10^{-6} m^2/s
Gas	Density	1.22 kg/m^3 (air)		1.20 kg/m^3 (N_2)
Injection Needle ID		0.22 mm		0.17 mm
Void Fraction Range		0 to 15 %		0 to 3 %
Bubble Radius Range		1.0 mm to 2.5 mm		0.5 mm to 1.0 mm
Bubble's Terminal Velocity in a Still Liquid Condition		0.10 m/s to 0.33 m/s (Involving Surfactant effect)		0.03 m/s to 0.12 m/s (No surfactant effect)

The bubble-illumination method (A) is available for the observation of void distribution whole field since every small bubble is captured into the video image by using the bubble's illumination angle. The illumination angle of a spherical air bubble in water is known about 115 degree so that in this experiment, the position of the used optical equipment is based on this angle.

The front-lighting method (B) is useful for visualizing liquid convection by using the surface tufts method. In this method, the tufts, 20 mm long are seamed on a thin brass plate in a lattice form. The brass plate is painted black and set on the internal wall of the tank. Of course, the tufts traceability, such as time response, is not able to detect the instantaneous flow but the average flow pattern of liquid phase can be easily identified.

The back-lighting method (C) is useful for quantitative image analysis since the size and the shape of the bubbles are exactly projected by the uniformly-diffused light source. The motion of each individual bubble is captured by using this lighting method and measured by particle imaging velocimetry.

2.2 Image Processing Method

Each recorded image is converted to a digital image data of 256 brightness levels (8 bit) and 510 × 480 pixels, and then processed to perform coordinate-matching, background reduction, noise reduction, and binarization. Time averaged void fraction is computed by summing the binarized image data for long enough term. Number density of bubble is calculated by counting the number of projected objects and the bubble size histogram is obtained from the object pixel number. For measuring the bubble velocity from the binarized image, the Binarized Image Cross Correlation method (BICC) is adopted. In this method, individual bubble velocity is computed on the basis of the distribution pattern similarity between two consecutive images of five local bubbles. By using this method, the velocities of more than 95% of the projected bubbles can be accurately obtained. For instance, more than 300 bubble velocity vectors are captured for every couple of consecutive images. Detailed principle and performance of this method are mentioned in previous papers, e.g. Uemura et al. (1990), Yamamoto et al. (1996).

3. Results and Discussion

3.1 Observation of a Swaying Bubble Plume

The basic behavior of the two-phase flow induced by the bubble plume is rather complex, but it can be basically described by the following processes. (1) the liquid inside the bubble plume is accelerated in the vertical direction by bubble buoyancy. (2) the velocity of the upward liquid flow decreases before reaching the top free surface. (3) the free surface level rises locally up just over the bubble plume. (4) at the free surface, the orientation of the liquid flow changes to the horizontal direction. (5) a strong horizontal flow or so-called "surface flow" is generated at the free surface. (6) the surface flow is dumped at the side walls and a downward flow occurs near them. (7) almost all the bubbles of the bubble plume are ejected during migration in the surface flow, but some of them are entrained by the downward flow. (8) the entrained bubbles continue to recirculate in the region where the bubble rising velocity and the liquid downward velocity are balanced. (9) the liquid which reaches the bottom region of the tank is again accelerated in the vertical direction by the bubble plume.

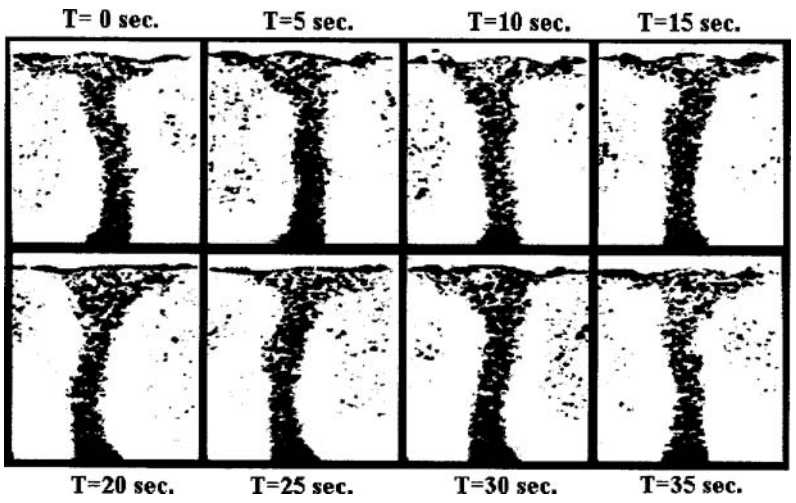

Fig. 2. Oscillatory inclining motion of an air bubble plume in water (initial free surface height: H = 300 mm, gas flow rate: $Q = 3.00 \times 10^{-5}$ m^3/s).

As an example, Figure 2 shows the negative image (i.e., black and white reversed image) of a time serial photographs of a bubble plume during 35 seconds. In these photographs, the size of the projected bubbles is larger than their real size because of the light scattering at the bubble surface. In this case, the flow field is practically square since the initial liquid height is equal to 300 mm. As seen in the figure, the bubble plume shows an oscillatory inclining motion in the horizontal direction. For this situation, the oscillatory period is about 50 seconds, i.e., the period of the oscillatory motion is much longer than the characteristic time which the bubble spends to rise from the injection point to the upper free surface (from 1 to 4 seconds). The plume swaying behavior occurs only for particular value of the gas flow rate, bubble size, water height, viscosity of liquid, and so on. Since this kind of flow instability may greatly affect the performance of practical industrial devices, it is important to better elucidate in the future the dynamic mechanism of this cyclic phenomenon.

A possible explanation of the described behavior could be the following one. If the plume slightly moves towards one side, the liquid there tends to be accelerated more than at the other side. Therefore, a lower pressure zone is initially established which further pushes the plume away from the centerline. However, the higher induced flow rate on this side can be delivered towards the surface only if, there, it develops a higher pressure which finally moves the plume towards the other side. Of course, this phenomenon has a little to do with the bubble rising time to free surface but it is rather dependent on the liquid motion and therefore on the liquid properties as well as the tank and injection zone geometries.

3.2 Calculation of Average Void Distribution

The time-averaged void distribution is qualitatively measured by image processing. In every case, time-averaging is performed over 128 seconds with an image sampling interval of 1.0 second.

For three different gas flow rates, Figure 3 represents at the top the instantaneous bubble pattern and at the bottom contours of time-averaged void distribution. The initial level of the free surface is 300 mm high, so that the aspect ratio is 1.00. The numbers which are noted in each contour mean the order of magnitude of the void. Therefore, the larger number indicates the larger void fraction. The following considerations arise from the results. (1) When the gas flow rate is low, all bubbles which are injected through the needles from the bottom plane, practically rise up straightly. Therefore, the bubble plume maintains its position steadily in the center part, its shape being a little inclined. (2) The bubble plume shows a periodically inclining motion when the gas flow rate is $Q = 3.00 \times 10^{-5}$ m^3/s. Owing to this behavior, the time-averaged void distribution is widely diffused in the medium part of the bubble plume. (3) At the highest gas flow rate, many bubbles are entrained under the free surface and remain in a region where balancing between bubble rising velocity and liquid downward velocity occurs. Owing to the symmetric buoyancy of these entrained bubbles, the oscillatory motion of the bubble plume disappears. Therefore, the time-averaged void distribution seems to correspond well to the instantaneous bubble distribution.

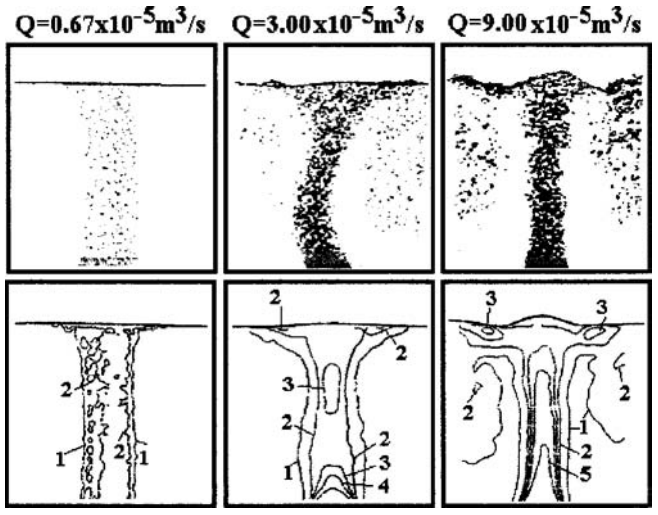

Fig. 3. Change of the air bubble plume in water with increase of gas flow rate for H = 300 mm.
(Top: instantaneous photograph, Bottom: contou of time-averaged void distribution)

For another testing condition Figure 4 represents results similar to those of Fig.3. In this case, water height is set at 600 mm so that the aspect ratio of initial water height to horizontal length is 2.00. Furthermore, the case for aspect ratio of 3.00 is shown in Fig.5. As shown by these figures, as the level of the free surface becomes higher, more meandering motions are observed in the rectangular tank. In a few cases, the time-averaged void distribution shows an asymmetrical profile. This occurrence and direct observation indicate that the relative arrangement of the steady vortices and the bubble plume is balanced but not symmetrically organized. As the gas flow rate increases, the upper part of the tank is occupied by a voidage layer which contains innumerable bubbles. In this region, liquid convection is no longer strongly induced because of the spatial uniformity of the void fraction.

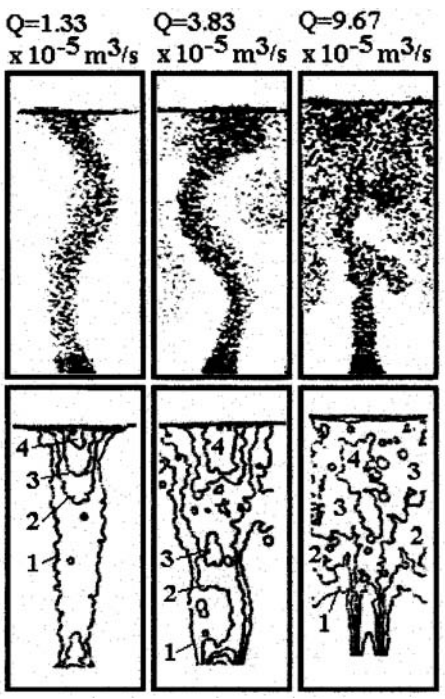

Fig. 4. Air bubble plume for H = 600 mm.

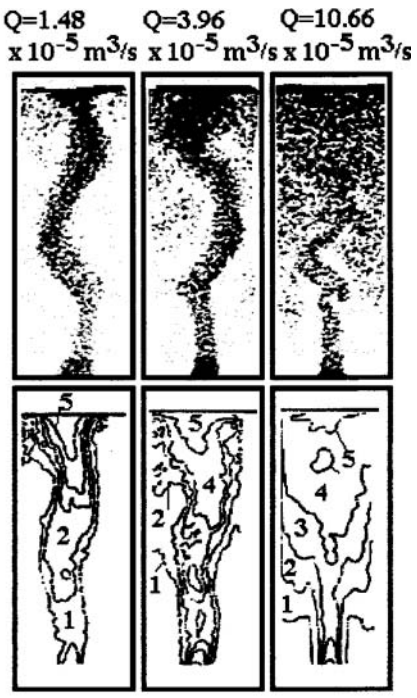

Fig. 5. Air bubble plume for H = 900 mm.

3.3 Visualization of Liquid Flow Pattern

Some photographs which are taken in order to visualize the flow pattern of liquid phase in the tank are shown in Fig.6 and Fig.7. In the case of aspect ratio equal to 1.00, as shown in Fig.6, the tufts indicate the presence of only one pair of large recirculation vortices. When the gas flow rate is higher, the bubbles entrained by the downward liquid flow accumulate in two small regions under the free surface, but images confirm that these regions do not have the same position of liquid vortex center. As shown in Fig.7, where the aspect ratio is 1.5, from three to four zones of liquid circulation develop. By direct observation, one may note that these liquid circulation zones change their position with a long period which is more than 30 seconds. This seems to indicate that the oscillatory motion of the bubble plume, which has the same long period, occurs due to the interaction between the bubble plume and the liquid convection.

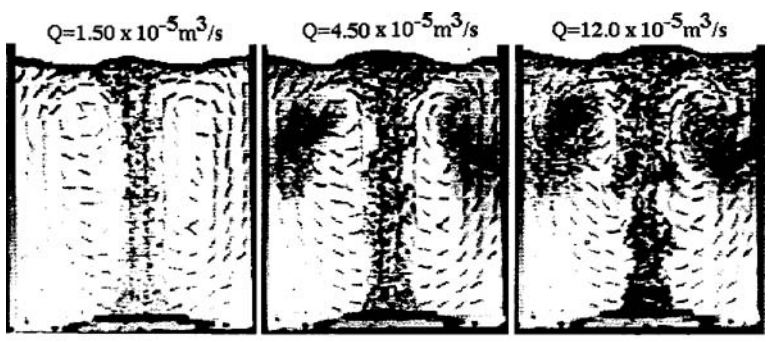

Fig. 6. Liquid flow pattern of air bubble plume in water for H = 300 mm.

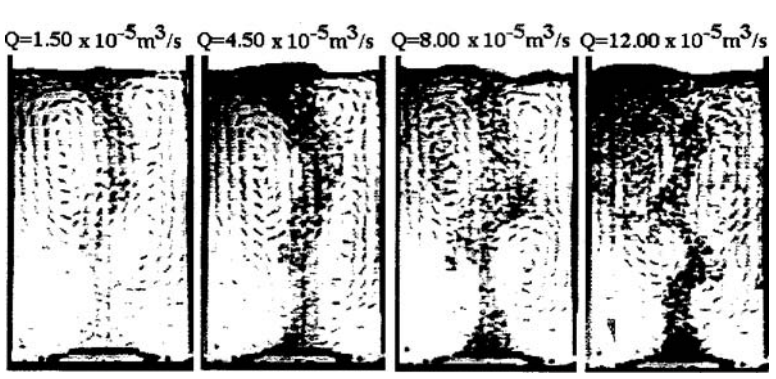

Fig. 7. Liquid flow pattern of air bubble plume in water rate for H = 450 mm

As reported by Alam and Arakeri (1993), there is another oscillatory motion of a bubble plume. They describe a sinuous instability of a plane bubble plume owing to the generation of strong shear stresses beside it. The main difference is that the bubble's size in this experiment is from about 2 to 4 mm, while in their experiment is smaller than 0.5 mm. In the case of small bubble's injection, the liquid receives a stronger buoyant force from the bubble due to the large resistance in slippery velocity between two phases.

3.4 Spatial Development of Bubble Number Density

Microscopic behavior of individual bubble motion along the plume is measured by applying the particle imaging velocimetry to dispersed bubbles. In these measurement, nitrogen gas is injected in silicone oil having a kinematic viscosity of 5 cSt. The level of the free surface is 600 mm (so, the aspect ratio is 2.0). For these conditions, the bubble plume does not show any oscillatory motion as shown in Fig.8, because liquid phase convection is not enough developed to interact with the bubble plume motion owing to the high viscosity. However, the local bubble motion in the bubble plume shows different type motion when the gas flow rate changes. The local instantaneous bubble distribution is shown in Fig.9. These are photographed at the three locations (L: low part, M: middle part, H: High part) which are indicated in Fig.1.

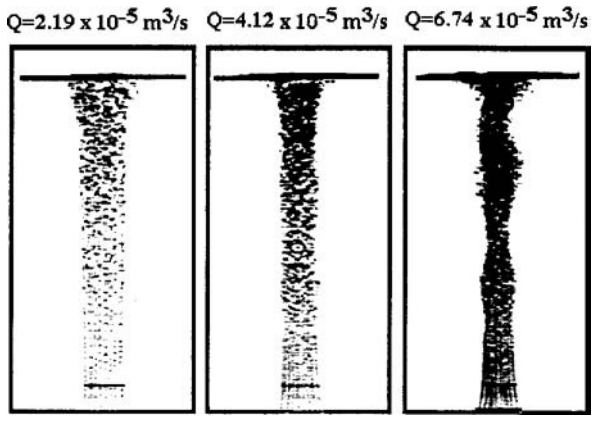

Fig. 8. Nitrogen gas bubble plume in silicon oil (kinematic viscosity is 5 cSt).

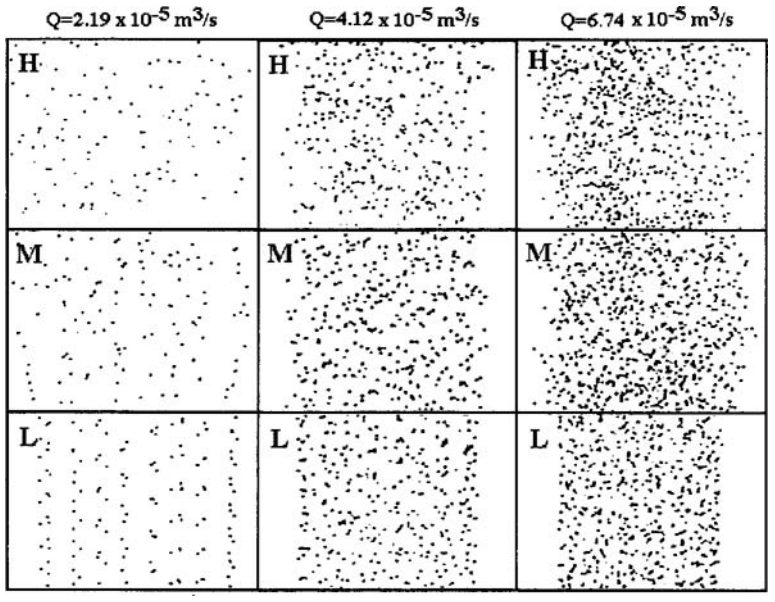

Fig. 9. Local bubble distribution in nitrogen gas bubble plume in silicon oil

In Fig.10, the horizontal profiles of the vertical bubble velocity and the bubble number density are presented. In the case of low gas flow rate, the initial profile of bubble number density, which depends on the arrangement of the bubble injection needles is practically maintained up to the upper region (High part). On the contrary, for the case of the high gas flow rate, the initial profile becomes smoother due to the mixing effect by bubble-induced turbulence. Furthermore, it changes to a profile which seems to have concentrated parts on the boundary regions of the bubble plume at the middle and the high parts. This occurs because certain effects of the lift force acting on bubble come out when the liquid is highly accelerated with strong shear velocity in the bubble plume. Generally, the diffusion process of a species concentration in a free jet, downstream obeys the Gaussian profile. By considering this matter, the present experimental results confirm that the spatial development process of the bubble number density profile is fundamentally different from a species diffusion process, but it depends on the particular characteristics of the translational motion of the bubbles.

3.5 Spatial Development of Bubble Rising Velocity

As shown in Fig.10, the vertical development of the bubble rising velocity is not so simple since this process is governed by the following phenomena.

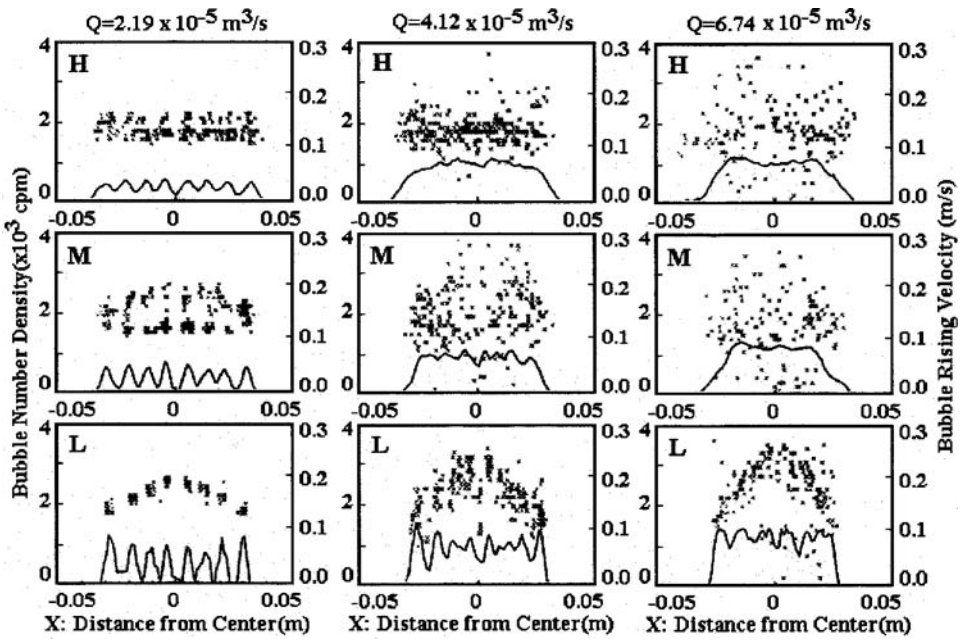

Fig. 10. Bubble number density and bubble rising velocity of N_2 bubble plume in silicon oil.
Nitrogen bubble plume in silicon oil, mean bubble radius is 1.0 mm. The oil has a kinematic viscosity of 5 cSt and a mass density of 960 kg/m^3. L (:106 mm), M (304 mm), L (504 mm) indicate the distance from the bubble injector to the height of the center of image processing frame. In each figure, points and lines show bubble rising velocity and bubble number density, respectively.

(1) By looking at the measured results in the low part, the vertical velocity of the bubble profile exhibits an almost parabolic shape for any gas flow rate. The velocity profile peak becomes sharper as the gas flow rate increases. The profile sharpening is due to the higher liquid rising velocity at the center axis of the bubble plume.

(2) For the case of small gas flow rate, the bubble rising velocity profile in the middle part seems to be separated into two different profiles, i.e., a parabolic profile and an almost uniform one. The velocity in the parabolic profile is larger than that in the uniform profile. This is due to a wall-effect that makes from 20 to 30 percent of the initially injected bubbles become so-called "wall-sliding bubbles." The reason why the sliding bubbles have an almost uniform profile is because the lift force on the bubbles is opposed by adhesion to the wall and because the liquid velocity has a high shear near the wall. The rising velocity of the sliding bubbles is lower than that of the other ones due to the large frictional force and lower liquid velocity at the wall. As shown by the relative diagram, in the high part, almost all the bubbles slide along the wall.

(3) As the gas flow rate increases, the bubble rising velocity profile in the high part exhibits such a large deviation that no longer, either parabolic or uniform, profile can be clearly distinguished. This is because each bubble motion has large fluctuations against the terminal rising velocity due to the local interaction with the liquid flow which becomes a turbulent-like structure. For example, the sliding bubbles can be ejected from the wall by the near-wall turbulence while the bubbles at the center part between the two walls are transportated to the near-walls by the lift force. However, such a flow structure in two-phase media is very difficult to be phenomenologically explained, so that it is expected to be comprehensively analyzed in the future.

4. Concluding Remarks

The overall, as well as individual, bubble in a plane bubble plume is investigated by means of both qualitative and quantitative flow visualization techniques. They include plume observation, measurement of time-averaged void distribution, surface tufts, and particle imaging velocimetry.

From this comprehensive set of measurements, the following conclusions can be described.

(1) The plane bubble plume in a tank can have a two-dimensional oscillatory behavior which period is much longer than the characteristic rising time of the bubble. The oscillatory pattern of the bubble plume is affected sensitively by the aspect ratio of the flow field, and by the kinematic viscosity of the liquid phase.
(2) By visualizing the liquid flow pattern using the tufts method, it is confirmed that the oscillatory motion is due to the interaction between the plume rising motion and several liquid vortices which are generated in the tank.
(3) By using particle imaging velocimetry for measuring the local bubble motion along the bubble plume zone, some detailed phenomena of the bubble rising process are found and discussed. In particular, relevance of the presence of wall-sliding bubbles and of the motion of a turbulent like structure have been captured.

Acknowledgments

The authors would like to thank Prof., Dr. Giovanni Maria Carlomagno for his advice and useful discussion on this topic. They are also grateful for the assistance provided by Dr. Nobuhiro Yamanishi at the Univ. of Tokyo for constructing image processing softwares.

References

Alam, M. and Arakeri, V. H., Observations on Transition in Plane Bubble Plumes, J. Fluid Mech., 254, (1993), 363-380.
Gross, R.W. and Kuhlman, J.M., Three-Component Velocity Measurements in a Laboratory Bubble Column, Proc. Int. Conf. Multiphase Flows '91-Tsukuba (1991), 157-162.
Hussain, N. A. and Siegel, R., Liquid Jet Pumped by Rising Gas Bubbles, J. Fluids Engng., March 8, (1976), 49-62.
Leitch, A. M. and Baines, W. D., Liquid Volume Flux in a Weak Bubble Plume, J. Fluid Mech., 205, (1989), 77-90.
McDouall, T. J., Bubble Plume in Stratified Environments, J. Fluid Mech., 85, (1978), 655-680.
Murai, Y. and Matsumoto, Y., Numerical Analysis of Detailed Flow Structures of a Bubble Plume, JSME International Journal, B, 41, 3, (1998), 568-575.
Murai, Y., Yamanishi, N. and Matsumoto, Y., Microscopic Behavior of the Bubble-Driven Convection, Proc. 3rd Asian Symp. Visualization, (Eds. Nakayama, Y. & Tanahashi, T.) (1994), 398-401.
Uemura, T., Yamamoto, F. and Koukawa, M., High-Speed Algorithm for Particle Tracking Velocimetry using Binary, J. Visualization Society of Japan, 10, 38, (1990), 58-64 (in Japanese).
Yamamoto, F., Wada, A., Iguchi, M. and Ishikawa, M., Discussion of the Cross-Correlation Methods for PIV, J. of Flow Visualization and Image Processing, 3,1 (1996), 65-78.

Author Profile

Yuichi Murai: He graduated from Ishikawa College of Technology in 1989 and received his BSc (Eng) degree in 1991 from Kanazawa University. He received Master degree (Eng) in 1993 and Doctor degree (Eng) in 1996 both from the University of Tokyo. He started a research on multiphase flow dynamics there while his main advisor was Professor Yoichiro Matsumoto, the 2nd author of this paper. After the Doctor degree he worked as a research associate in the group of thermo-fluid engineering of Fukui University, especially for the bubbly two-phase flow. His current research interest is applications of PIV technique to multiphase flow unknowns.

Yoichiro Matsumoto: He received his BSc (Eng) degree in 1972 and Doctor degree of Engineering in 1977 in mechanical engineering from the University of Tokyo. After Doctor degree he worked mainly in cavitation and multiphase flow analysis with Professor Hideo Ohashi. He became a professor at the University of Tokyo in 1993 and currently investigates on various interfacial phenomena by means of direct numerical simulations, multiphase flow modeling, molecular dynamics, LDV, and PIV.

Fujio Yamamoto: He received his BSc (Eng) degree in 1963 from Fukui University and Master (Eng) degree in 1965 from Osaka University. He worked as a researcher at Sumitomo Heavy Industries, Co, LTD from 1966 to 1969, and received Doctor degree of Engineering in 1979 from Osaka University. He become a professor in 1991. His interest in last ten years was to develop PIV techniques and their application to multiphase flow. He received the Prize for Distinguished Service from the Visualization Society of Japan in 1992.